



HAL
open science

Determination of transport parameters in air-saturated porous materials via reflected ultrasonic waves

Zine El Abiddine Fellah, C Depollier, S Berger, W Lauriks, P Trompette, J-Y Chapelon

► **To cite this version:**

Zine El Abiddine Fellah, C Depollier, S Berger, W Lauriks, P Trompette, et al.. Determination of transport parameters in air-saturated porous materials via reflected ultrasonic waves. *Journal of the Acoustical Society of America*, 2003, 114, pp.2561 - 2569. 10.1121/1.1621393 . hal-04230400

HAL Id: hal-04230400

<https://hal.science/hal-04230400>

Submitted on 5 Oct 2023

HAL is a multi-disciplinary open access archive for the deposit and dissemination of scientific research documents, whether they are published or not. The documents may come from teaching and research institutions in France or abroad, or from public or private research centers.

L'archive ouverte pluridisciplinaire **HAL**, est destinée au dépôt et à la diffusion de documents scientifiques de niveau recherche, publiés ou non, émanant des établissements d'enseignement et de recherche français ou étrangers, des laboratoires publics ou privés.

Determination of transport parameters in air-saturated porous materials via reflected ultrasonic waves

Z. E. A. Fellah^{a)}

National Institute of Health and Medical Research (INSERM U556), 151 cours Albert Thomas, 69424 Lyon Cedex 03, France

C. Depollier

Laboratoire d'Acoustique de l'Université du Maine, UMR-CNRS 6613, Université du Maine, Avenue Olivier Messiaen, 72085 Le Mans Cedex 09, France

S. Berger and W. Lauriks

Laboratorium voor Akoestiek en Thermische Fysica, Katholieke Universiteit Leuven, Celestijnenlaan 200 D, B-3001 Heverlee, Belgium

P. Trompette and J.-Y. Chapelon

National Institute of Health and Medical Research (INSERM U556), 151 cours Albert Thomas, 69424 Lyon Cedex 03, France

(Received 22 May 2003; revised 9 August 2003; accepted 2 September 2003)

An ultrasonic reflectivity method of evaluating the acoustic parameters of porous materials saturated by air (or any other gas) is discussed. The method is based on experimental detection of waves reflected at normal incidence by the first and second interface of the material. This method is based on a temporal model of direct and inverse scattering problems for the propagation of transient ultrasonic waves in a homogeneous isotropic slab of porous material with a rigid frame [Fellah *et al.*, *J. Acoust. Soc. Am.* **113**, 61–73 (2003)]. Generally, the conventional ultrasonic approach can be used to determine tortuosity, and viscous and thermal characteristic lengths via transmitted waves. Porosity cannot be estimated in transmitted mode because of its very weak sensitivity. First interface use of the reflected wave at oblique incidence leads to the determination of porosity and tortuosity [Fellah *et al.*, *J. Acoust. Soc. Am.* **113**, 2424–2433 (2003)] but this is not possible at normal incidence. Using experimental data of reflected waves by the first and second interface at normal incidence simultaneously leads to the determination of porosity, tortuosity, viscous and thermal characteristic lengths. As with the classic ultrasonic approach for characterizing porous material saturated with one gas, both characteristic lengths are estimated individually by assuming a given ratio between them. Tests are performed using weakly resistive industrial plastic foams. Experimental and numerical results, and prospects are discussed. © 2003 Acoustical Society of America. [DOI: 10.1121/1.1621393]

PACS numbers: 43.20.Bi, 43.20.Hq [ANN]

Pages: 2561–2569

I. INTRODUCTION

The propagation of sound in fluid-saturated porous media with rigid solid frames is of great interest for a wide range of industrial applications. With air as the pore fluid,^{1–3} applications can be found in noise control, nondestructive material characterization, thermoacoustically controlled heat transfer, etc.

Many applications, such as medical imaging or inverse scattering, require a study of the behavior of pulses traveling into porous media. When a broadband ultrasound pulse passes through a layer of a medium, the pulse wave form changes as a result of attenuation and dispersion of the medium. The classic method for predicting a change in the wave form of a signal passing through a medium relies on the system's impulse response. According to the theory of linear systems, the output signal is a convolution of the input signal and the system impulse response. Many media, in-

cluding porous materials and soft tissues, have been observed to have an attenuation function that increases with frequency. As a result, higher frequency components of the pulse are attenuated more than lower frequency components. After passing through the layer, the transmitted pulse is not just a scaled down version of the incident pulse, but has a different shape. Dispersion refers to the phenomenon observed when the phase velocity of a propagating wave changes with frequency. Dispersion causes the propagating pulse wave form to change because wave components with different frequencies travel at different speeds. An understanding of the interaction of ultrasound with a porous medium in both time and frequency domains, and the ability to determine the change of wave form when propagating ultrasound pulses, should be useful in designing array transducers and in quantitative ultrasound tissue characterization.

To cope efficiently with the specific problems appearing in transient acoustic field propagation, new approaches are required.^{4,5} At present, most analyses of signal propagation are carried out in the frequency domain using the Fourier

^{a)}Electronic mail: fellah@lyon.inserm.fr

transform, and the results are translated to the time domain, and vice-versa. However this has several limitations. The first is that the transformation is difficult to compute accurately enough numerically for nonanalytical functions. For example, using the Fourier transform to obtain time domain results for a lossy material is a more complicated approach than using true time domain analysis, and the numerical results are less accurate. The second disadvantage is that by working in the frequency domain, some numerical information is lost or hard to recover. For example, in the case of noisy data it may be difficult to reconstruct the chronological events of a signal by phase unwrapping. Consequently, it is difficult to obtain a deep understanding of transient signal propagation using the frequency domain method.

A time domain approach differs from a frequency analysis in that the susceptibility functions describing viscous and thermal effects are convolution operators acting on velocity and pressure, and therefore a different algebraic formalism must be applied to solve the wave equation. The time domain response of the material is described by an instantaneous response and a “susceptibility” kernel responsible for memory effects. The attraction of a time domain based approach is that analysis is naturally bounded by the finite duration of ultrasonic pressures and is consequently the most appropriate approach for the transient signal.

In this work, we present a reflectivity method for measuring the physical parameters describing the propagation of ultrasonic pulses in air-saturated porous materials. This method is based on a temporal model of direct and inverse scattering problems for the propagation of transient ultrasonic waves in a homogeneous isotropic slab of porous material with a rigid frame, initially introduced by the authors.⁶ The principle of this method is to measure the wave reflected by the first and second interface of a slab of porous material, and to solve the inverse problem in order to estimate the physical parameters (porosity, tortuosity, viscous and thermal characteristic lengths). The advantage of this method over classic ultrasonic methods is that all these parameters can be determined simultaneously using experimental reflected data (the ratio between the viscous and thermal characteristic lengths is fixed as in classical acoustical methods^{7,8}).

The outline of this paper is as follows. Section II recalls a time domain model and the basic equations of wave propagation in porous material. Section III is devoted to the direct problem and the expression of reflection and transmission kernels in the time domain at normal incidence. In Sec. IV, the sensitivity of porosity and tortuosity, as well as viscous and thermal characteristic lengths are discussed, showing the effect of each parameter on the waves reflected by the first and second interface. Section V contains the inverse problem and the appropriate procedure, based on the least square method, which is used to estimate the acoustic parameters. Finally in Sec. VI, experimental validation using ultrasonic measurement is discussed for air-saturated industrial plastic foams.

II. MODEL

In porous material acoustics, a distinction can be made between two situations depending on whether the frame is

moving or not. In the first case, the wave dynamics due to coupling between the solid frame and the fluid are clearly described by the Biot theory.^{9,10} In air-saturated porous media, the structure is generally motionless and the waves propagate only in the fluid. This case is described by the equivalent fluid model which is a particular case in the Biot model, in which fluid-structure interactions are taken into account in two frequency response factors: dynamic tortuosity of the medium $\alpha(\omega)$ given by Johnson *et al.*¹¹ and dynamic compressibility of the air in the porous material $\beta(\omega)$ given by Allard.¹ In the frequency domain, these factors multiply the fluid density and compressibility, respectively, and show the deviation from fluid behavior in free space as frequency increases. In the time domain, they act as operators and in the asymptotic domain (high frequency approximation) their expressions are given^{4,6} by

$$\tilde{\alpha}(t) = \alpha_\infty \left(\delta(t) + \frac{2}{\Lambda} \left(\frac{\eta}{\pi \rho_f} \right)^{1/2} t^{-1/2} \right), \quad (1)$$

$$\tilde{\beta}(t) = \left(\delta(t) + \frac{2(\gamma-1)}{\Lambda'} \left(\frac{\eta}{\pi \text{Pr} \rho_f} \right)^{1/2} t^{-1/2} \right). \quad (2)$$

In these equations, $\delta(t)$ is the Dirac function, $\text{Pr}=0.71$ is the Prandtl number, $\eta=1.84 \cdot 10^{-5} \text{ kg m s}^{-1}$ and $\rho_f=1.23 \text{ kg m}^{-3}$ are, respectively, fluid viscosity and fluid density, and $\gamma=1.4$ is the adiabatic constant. The relevant physical parameters of the model are the medium tortuosity α_∞ , and viscous and thermal characteristic lengths Λ and Λ' . In this model the time convolution of $t^{-1/2}$ with a function is interpreted as a semi-derivative operator according to the definition of the fractional derivative of order ν given in Samko *et al.*¹²

$$D^\nu[x(t)] = \frac{1}{\Gamma(-\nu)} \int_0^t (t-u)^{-\nu-1} x(u) du, \quad (3)$$

where $\Gamma(x)$ is the gamma function.

In this framework, the basic equations^{4,6} for our model can be written as

$$\rho_f \tilde{\alpha}(t) * \frac{\partial v_i}{\partial t} = -\nabla_i p, \quad \tilde{\beta}(t) * \frac{\partial p}{\partial t} = -\nabla \cdot \mathbf{v}, \quad (4)$$

where $*$ denotes the time convolution operation, p is acoustic pressure, \mathbf{v} is particle velocity, and $K_a=141\,820 \text{ Pa}$ is the bulk modulus of air. The first equation is the Euler equation, the second one is the constitutive equation.

For a wave propagating along the x axis, these equations become

$$\begin{aligned} \rho_f \alpha_\infty \frac{\partial v(x,t)}{\partial t} + 2 \frac{\rho_f \alpha_\infty}{\Lambda} \left(\frac{\eta}{\pi \rho_f} \right)^{1/2} \int_0^t \frac{\partial v(x,t')/\partial t'}{\sqrt{t-t'}} dt' \\ = -\frac{\partial p(x,t)}{\partial x}, \end{aligned} \quad (5)$$

$$\begin{aligned} \frac{1}{K_a} \frac{\partial p(x,t)}{\partial t} + 2 \frac{\gamma-1}{K_a \Lambda'} \left(\frac{\eta}{\pi \text{Pr} \rho_f} \right)^{1/2} \int_0^t \frac{\partial p(x,t')/\partial t'}{\sqrt{t-t'}} dt' \\ = -\frac{\partial v(x,t)}{\partial x}. \end{aligned} \quad (6)$$

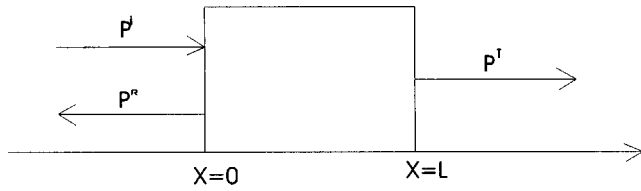


FIG. 1. Problem geometry.

In these equations, the convolutions express the dispersive nature of the porous material. They take into account the memory effects due to the fact that the medium's response to wave excitation is not instantaneous but needs more time to take effect.

The generalized lossy wave equation in the time domain is derived from the basic equations (5) and (6) by elementary calculation as follows:

$$\frac{\partial^2 p(x,t)}{\partial x^2} - A \frac{\partial^2 p(x,t)}{\partial t^2} - B \int_0^t \frac{\partial^2 p(x,t)/\partial t'^2}{\sqrt{t-t'}} dt' - C \frac{\partial p(x,t)}{\partial t} = 0, \quad (7)$$

where coefficients A , B , and C are constants given by

$$A = \frac{\rho_f \alpha_\infty}{K_a}, \quad B = \frac{2\alpha_\infty}{K_a} \sqrt{\frac{\rho_f \eta}{\pi}} \left(\frac{1}{\Lambda} + \frac{\gamma-1}{\sqrt{\text{Pr}} \Lambda'} \right), \quad (8)$$

$$C = \frac{4\alpha_\infty(\gamma-1)\eta}{K_a \Lambda \Lambda' \sqrt{\text{Pr}}},$$

respectively. The first one concerns the velocity $c = 1/\sqrt{\rho_f \alpha_\infty / K_a}$ of the wave in the air in the porous material. α_∞ gives the refractive index of the medium which changes the wave velocity from $c_0 = \sqrt{K_a / \rho_f}$ in free space to $c = c_0 / \sqrt{\alpha_\infty}$ in the porous medium. The other coefficients essentially depend on the characteristic lengths Λ and Λ' and express fluid-structure viscous and thermal interactions. The constant B governs signal spreading while C is responsible for wave attenuation.

III. DIRECT PROBLEM

The direct scattering problem involves determining the scattered field as well as the internal field, arising when a known incident field impinges on a porous material with known physical properties. Green's function¹³ for the modified wave equation in the porous medium must be known in order to compute a solution for the direct problem. In that case, the internal field is given by the time convolution for Green's function with the incident wave, and the reflected and transmitted fields are deduced from the internal field and boundary conditions.

In this section some notation is introduced. The problem geometry is given in Fig. 1. A homogeneous porous material occupies region $0 \leq x \leq L$. This medium is assumed to be isotropic and to have a rigid frame. A short sound pulse impinges normally on the medium from the left. It generates an acoustic pressure field $p(x,t)$ and an acoustic velocity field $v(x,t)$ within the material, which satisfy Eqs. (5) and (6).

To derive the reflection and transmission scattering operators, it is assumed that the pressure field and flow velocity are continuous at the material boundary,

$$p(0^+, t) = p(0^-, t), \quad p(L^-, t) = p(L^+, t), \quad (9)$$

$$v(0^-, t) = \phi v(0^+, t), \quad v(L^+, t) = \phi v(L^-, t),$$

where ϕ is the porosity of the medium and the positive and negative superscript denotes the limit from left and right, respectively. Assumed initial conditions are

$$p(x,t)|_{t=0} = 0, \quad \frac{\partial p}{\partial t} \Big|_{t=0} = 0, \quad (10)$$

which means that the medium is idle for $t=0$.

If the incident sound wave is generated in region $x \leq 0$, then the expression of the acoustic field in the region to the left of the material is the sum of the incident and reflected fields,

$$p_1(x,t) = p^i \left(t - \frac{x}{c_0} \right) + p^r \left(t + \frac{x}{c_0} \right), \quad x < 0. \quad (11)$$

Here, $p_1(x,t)$ is the field in the region $x < 0$, p^i and p^r denote the incident and reflected fields, respectively. In addition, a transmitted field is produced in the region to the right of the material. This has the form

$$p_3(x,t) = p^t \left(t - \frac{L}{c} - \frac{(x-L)}{c_0} \right), \quad x > L. \quad (12)$$

[$p_3(x,t)$ is the field in region $x > L$ and p^t is the transmitted field.]

The incident and scattered fields are related by scattering operators (i.e., reflection and transmission operators) for the material. These are integral operators represented by

$$p^r(x,t) = \int_0^t \tilde{R}(\tau) p^i \left(t - \tau + \frac{x}{c_0} \right) d\tau$$

$$= \tilde{R}(t) * p^i(t) * \delta \left(t + \frac{x}{c_0} \right), \quad (13)$$

$$p^t(x,t) = \int_0^t \tilde{T}(\tau) p^i \left(t - \tau - \frac{L}{c} - \frac{(x-L)}{c_0} \right) d\tau$$

$$= \tilde{T}(t) * p^i(t) * \delta \left(t - \frac{L}{c} - \frac{(x-L)}{c_0} \right). \quad (14)$$

In Eqs. (13) and (14) functions \tilde{R} and \tilde{T} are the reflection and transmission kernels, respectively, for incidence from the left. Note that the lower limit of integration in Eqs. (13) and (14) is given as 0, which is equivalent to assuming that the incident wave front first impinges on the material at $t=0$. The operators \tilde{R} and \tilde{T} are independent of the incident field used in the scattering experiment and depend only on the properties of the materials.

Using boundary and initial conditions (9) and (10), reflection and transmission scattering operators can be derived,⁶ taking into account the n -multiple reflections in the material:

$$\tilde{R}(t) = \left(\frac{1-E}{1+E} \right) \sum_{n \geq 0} \left(\frac{1-E}{1+E} \right)^{2n} \left[F \left(t, 2n \frac{L}{c} \right) - F \left(t, (2n+2) \frac{L}{c} \right) \right], \quad (15)$$

$$\tilde{T}(t) = \frac{4E}{(1+E)^2} \sum_{n \geq 0} \left(\frac{1-E}{1+E} \right)^{2n} F \left(t + \frac{L}{c}, (2n+1) \frac{L}{c} \right). \quad (16)$$

In these equations, $E = \phi / \sqrt{\alpha_\infty}$ and F are the medium's Green function¹³ given by

$$F(t, k) = \begin{cases} 0 & \text{if } 0 \leq t \leq k \\ \Xi(t) + \Delta \int_0^{t-k} h(t, \xi) d\xi & \text{if } t \geq k \end{cases} \quad (17)$$

with

$$\Xi(t) = \frac{b'}{4\sqrt{\pi}} \frac{k}{(t-k)^{3/2}} \exp\left(-\frac{b'^2 k^2}{16(t-k)}\right), \quad (18)$$

where $h(\tau, \xi)$ has the following form:

$$h(\tau, \xi) = -\frac{1}{4\pi^{3/2}} \frac{k}{\sqrt{(\tau-\xi)^2 - k^2}} \frac{1}{\xi^{3/2}} \times \int_{-1}^1 \exp\left(-\frac{\chi(\mu, \tau, \xi)}{2}\right) (\chi(\mu, \tau, \xi) - 1) \frac{\mu d\mu}{\sqrt{1-\mu^2}} \quad (19)$$

and where $\chi(\mu, \tau, \xi) = (\Delta\mu\sqrt{(\tau-\xi)^2 - k^2} + b'(\tau-\xi))^2 / 8\xi$, $b' = Bc_0^2\sqrt{\pi}$, $c' = C \cdot c_0^2$ and $\Delta^2 = b'^2 - 4c'$.

In most cases of air-saturated porous materials, multiple reflection effects may be negligible because of the high attenuation of sound waves in these media. This depends on the thickness L and physical properties of the porous material. For porous material with high flow resistivity, only the wave reflected by the first interface is seen experimentally and all other reflection contributions are neglected. So, by taking into account only the first reflections at interfaces $x=0$ and $x=L$, the expression of the reflection operator will be given by

$$\tilde{R}(t) = r(t) + \mathfrak{R}(t), \quad (20)$$

with

$$r(t) = \left(\frac{1-E}{1+E} \right) \delta(t), \quad \mathfrak{R}(t) = -\frac{4E(1-E)}{(1+E)^3} F \left(t, \frac{2L}{c} \right). \quad (21)$$

$r(t)$ is the instantaneous response of the porous material corresponding to the reflection contribution at the first interface ($x=0$). $\mathfrak{R}(t)$ is equivalent to reflection at the second interface $x=L$. The part of the wave corresponding to $r(t)$ is not subjected to dispersion but simply multiplied by the factor

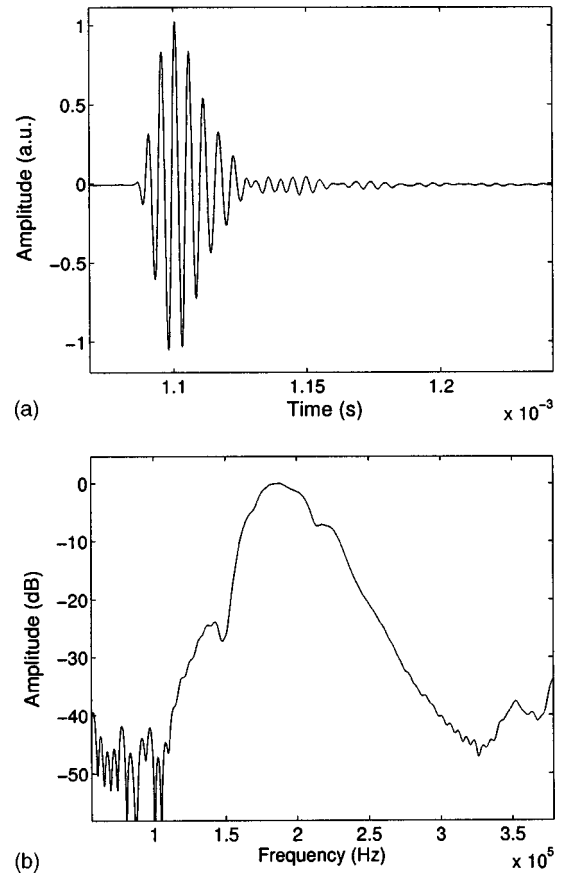


FIG. 2. (a) Incident signal. (b) Spectrum of the incident signal.

$(1-E)/(1+E)$. The experimental detection of the reflection contribution by the second interface depends strongly on the sample's thickness and acoustic properties (porosity, tortuosity, viscous and thermal characteristic lengths). It may be interesting to be able to measure the second reflection contribution, because it could offer an alternative method for determining acoustic parameters which are now measured acoustically only in transmission mode.⁶ In fact the wave reflected by the second interface depends on the medium's Green function F which is expressed in terms of the ultrasonic parameters. This wave is diffusive compared to the wave reflected by the first interface.

IV. ACOUSTIC PARAMETER SENSITIVITY

In this section, numerical simulations of waves reflected by a slab of porous material are run by varying the independent geometrical parameters of a porous medium described acoustically using the theory developed in Sec. III. 50% variation is applied to the governing parameters. A first numerical simulation is produced. The incident signal used in the simulation is given in Fig. 2(a). Its spectrum is given in Fig. 2(b). The numerical values chosen for the physical parameters correspond to quite common acoustic materials, as follows: thickness $L=1$ cm, tortuosity $\alpha_\infty=1.05$, viscous characteristic length $\Lambda=300 \mu\text{m}$, thermal characteristic length $\Lambda'=900 \mu\text{m}$, and porosity $\phi=0.97$. The result of the simulation is a signal as shown in Fig. 3(a). Amplitude is given by an arbitrary unit and the point number given in the

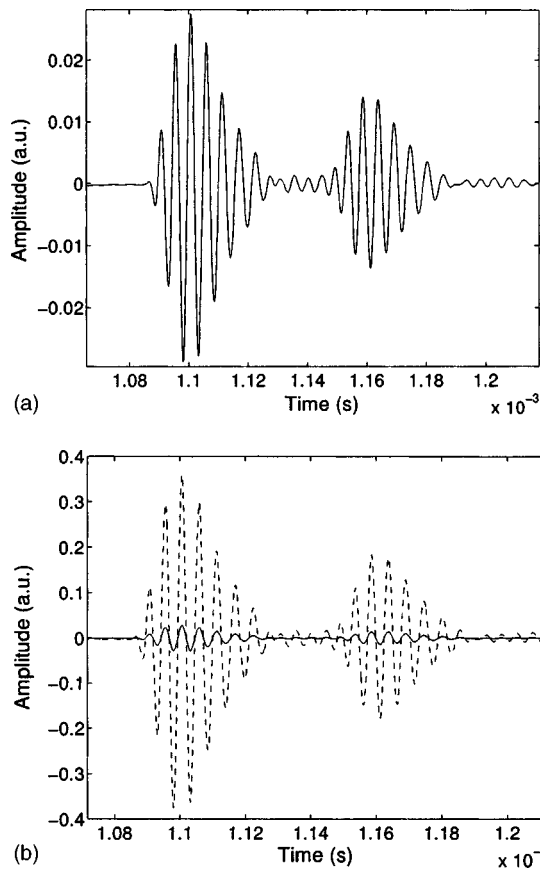


FIG. 3. (a) Simulated reflected signal. (b) Comparison between simulated reflected signals corresponding to $\phi=0.97$ (solid line) and $\phi=0.48$ (dashed line).

abscissa is proportional to time. In Fig. 3, the two signals correspond to the waves reflected by the first and second interface, respectively. The speed of the first wave is the speed of free air 340 m s^{-1} and the speed of the second wave, which propagates inside the porous material, is 331 m s^{-1} ($c=c_0/\sqrt{\alpha_\infty}$).

Figure 3(b) shows the results obtained after reducing porosity by 50% of its initial value. The first signal (solid line) corresponds to the simulated reflected signal for $\phi=0.97$ and the second one (dashed line) to $\phi=0.48$. The values of the other parameters have been kept constant ($L=1 \text{ cm}$, $\alpha_\infty=1.05$, $\Lambda=300 \mu\text{m}$, and $\Lambda'=900 \mu\text{m}$). The sensitivity of porosity in reflected mode can be seen for a 50% change. There is an important change of amplitude in the two waves (first and second interface). By reducing porosity, the amplitudes of the wave reflected by the first and second interface increase by 775% and 800% of their initial values, respectively. This result can be predicted by the fact that when porosity decreases, the porous material becomes very resistive and the incident wave is then more reflected by the porous material.

When the thickness decreases by 50% of its initial value, the reflected signal also changes. The values of the ultrasonic parameters have been kept constant ($\alpha_\infty=1.05$, $\phi=0.97$, $\Lambda=300 \mu\text{m}$, $\Lambda'=900 \mu\text{m}$). Figure 4 shows a comparison of two reflected signals with two different thicknesses. The first one (solid line) corresponds to a thickness of 1 cm and the second one (dashed line) to 0.5 cm. By reducing the thick-

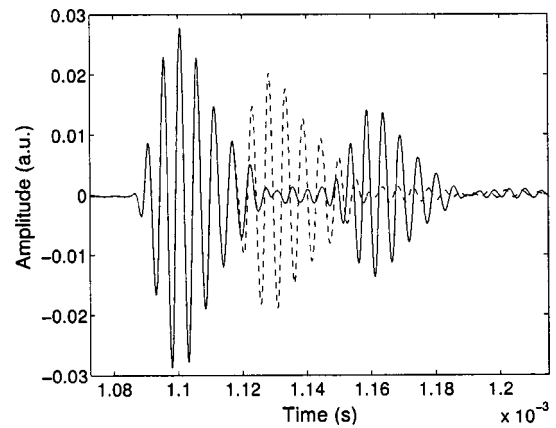


FIG. 4. Comparison between simulated reflected signals corresponding to $L=1 \text{ cm}$ (solid line) and $L=0.5 \text{ cm}$ (dashed line).

ness of the material, the distance propagated by the second reflected wave in the porous material falls and is less attenuated. It leads to an increase of amplitude of 40% of its initial value in the second reflected wave.

Now let us look at the effect of tortuosity. Figure 5 shows a comparison of two simulated reflected signals, the first (solid line) corresponding to $\alpha_\infty=1.05$ and the second (dashed line) to $\alpha_\infty=1.57$. In this simulation, the values of the thickness, porosity, viscous and thermal characteristic lengths have been kept constant ($L=1 \text{ cm}$, $\Lambda=300 \mu\text{m}$, $\Lambda'=900 \mu\text{m}$, and $\phi=0.97$). From the two signals of Fig. 5, it can be seen that tortuosity plays an important part in reflected waves. By increasing the value of tortuosity, the speed of the wave reflected by the second interface has fallen from 331 to 270 m s^{-1} . However, the amplitude of the two waves increases, the wave reflected by the first interface increases by 420% of its initial amplitude and the wave reflected by the second interface increases by 250% of its initial amplitude. On increasing tortuosity, the inertial couplings between fluid and structure also increase, the porous material becomes more resistive, and then the reflected operators [Eq. (21)] of the first and second interface increase. At the same time, the wave reflected by the second interface is much delayed and its amplitude is less amplified compared with the wave reflected by the first interface. This can be ex-

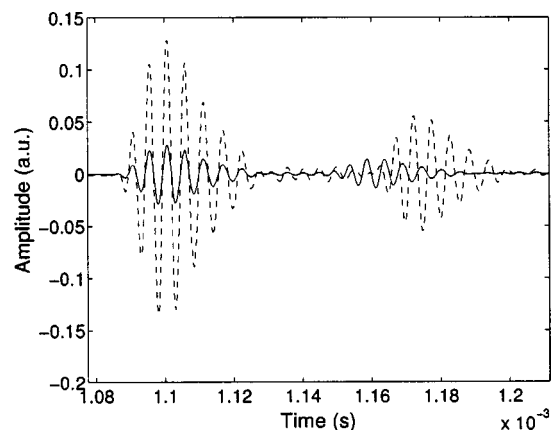


FIG. 5. Comparison between simulated reflected signals corresponding to $\alpha_\infty=1.05$ (solid line) and $\alpha_\infty=1.57$ (dashed line).

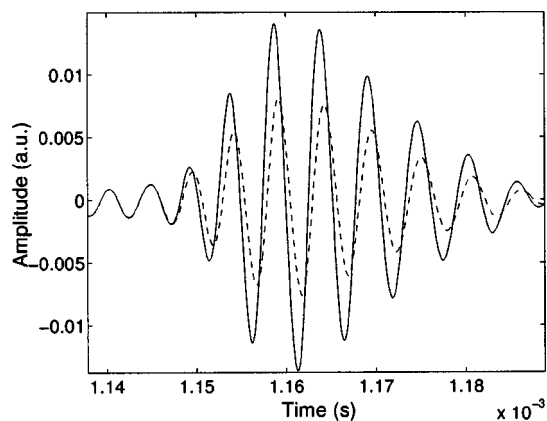


FIG. 6. Comparison between simulated reflected signals at the second interface corresponding to $\Lambda=300 \mu\text{m}$ (solid line) and $\Lambda=150 \mu\text{m}$ (dashed line).

plained by additional inertial losses in the second reflected wave due to the propagation phenomenon.

Figure 6 shows the sensitivity of viscous characteristic length Λ on the reflected wave by the second interface (the reflected wave by the first interface is not affected by Λ). The signal plotted as a solid line corresponds to $\Lambda=300 \mu\text{m}$ and the dashed line transmitted signal to $\Lambda=150 \mu\text{m}$. The values of the other parameters have been kept constant ($L=1 \text{ cm}$, $\alpha_\infty=1.05$, $\Lambda'=900 \mu\text{m}$, and $\phi=0.97$). It can be seen that the amplitude of the reflected wave by the second interface has fallen by 85% of its initial value. A very small change occurs at the speed of the wave reflected by the second interface due to the dispersion phenomenon governed by Λ . This length appears in the second term in the asymptotic expression of dynamic tortuosity at high frequencies [Eq. (1)], and as shown by this numerical simulation, Λ plays a less important role in reflected waves than tortuosity, which appears in the first order of expression of the tortuosity operator $\tilde{\alpha}(t)$ [Eq. (1)]. In transmission mode, viscous characteristic length plays an important role in dispersion, especially for resistive porous materials.

Figure 7 shows a comparison of two simulated reflected signals corresponding to two different thermal characteristic lengths Λ' (only the reflected wave by the second interface is

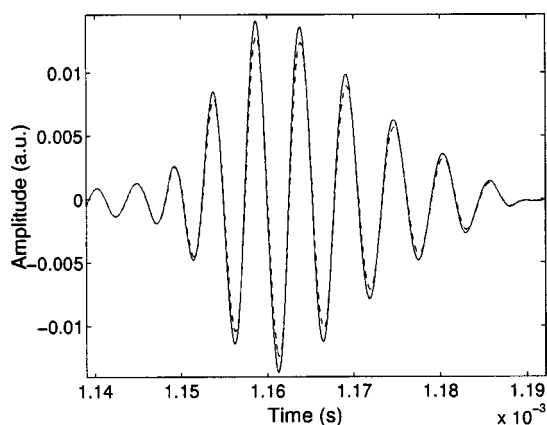


FIG. 7. Comparison between simulated reflected signals at the second interface corresponding to $\Lambda'=900 \mu\text{m}$ (solid line) and $\Lambda'=450 \mu\text{m}$ (dashed line).

presented in Fig. 7, the reflected wave by the first interface is not affected by Λ'). The first one (solid line) corresponds to $\Lambda'=900 \mu\text{m}$ and the second one (dashed line) to $\Lambda'=450 \mu\text{m}$. A small change is only observed in the wave reflected by the second interface, in which its amplitude has fallen by 8% of its initial value.

From this study, we can gain an insight into the sensitivity of each physical parameter used in this theory. The parameters which are involved in propagation and dispersion phenomena such as viscous and thermal characteristic lengths Λ and Λ' are only involved in the wave reflected by the second interface wave form. This wave propagates inside the porous material and is thus subjected to viscous and thermal interactions between fluid and structure, responsible for damping the acoustic wave in porous material. However, the wave reflected by the first interface is immediately reflected by the material and does not propagate inside the porous medium. This wave is not sensitive to parameters describing dispersion phenomena such as Λ and Λ' .

We also note from these simulations that some parameters such as porosity ϕ , tortuosity α_∞ , and thickness play an important role simultaneously in both waves reflected by the first and second interface wave forms compared to other parameters which act on the wave form of just one of the two waves.

V. INVERSE PROBLEM

The propagation of acoustic waves in a slab of porous material in the asymptotic domain is characterized by four parameters, namely, porosity ϕ , tortuosity α_∞ , viscous characteristic length Λ , and thermal characteristic length Λ' , the values of which are crucial for the behavior of sound waves in such materials. So, it is of some importance to develop new experimental methods and efficient tools for their estimation. Therefore, a basic inverse problem associated with the slab may be stated as follows: by measuring signals transmitted and/or reflected outside the slab, find the values of the medium's parameters. The inverse problem has been solved in transmission mode in Ref. 6 and an estimate of α_∞ , Λ , and Λ' has been made, giving a good correlation between experiment and theory. Porosity has not been estimated in transmitted mode because of its very weak sensitivity. The inverse problem for reflected waves has been solved only for the wave reflected by the first interface at oblique incidence, giving good results for tortuosity and porosity in plastic foams.¹⁴ The determination of porosity and tortuosity is not possible at normal incidence from the reflected wave at the first interface. Viscous and thermal characteristic lengths have not been estimated, because they do not depend on the wave reflected by the first interface. It may be interesting to develop a method to measure all the parameters in one mode (reflection or transmission), although it seems to be impossible in transmitted mode.⁶ However for weakly resistive porous materials, such as some plastic foams and fibrous materials, it may be possible to detect the wave reflected by the second interface experimentally, and this gives the same physical information as the transmitted wave, so we can then hope to use these experimental data (waves reflected by the first and second interface) to estimate

all the physical parameters describing propagation. A study of the sensitivity of the physical parameters involved in the reflected signal shows that it may be possible to obtain the effect of each parameter in one or two reflected waves.

As shown in Sec. V, solution of the direct problem involves a system of two operators expressed as functions of ϕ , α_∞ , Λ , and Λ' . The inversion algorithm for finding the values of the slab parameters in reflected mode is based on an appropriate procedure: find the values of the parameters ϕ , α_∞ , Λ , and Λ' such that the reflected signal describes the scattering problem in the best possible way (e.g., in the least-squares sense). Because of the weak sensitivity of Λ' in the porous material's reflected response, the Λ'/Λ ratio is set to 3 (Λ'/Λ is classically set from 2 to 3 for plastic foams^{7,8}).

The inverse problem is to find values for parameters ϕ , α_∞ , and Λ which minimize the function

$$U(\phi, \alpha_\infty, \Lambda) = \int_0^t (p_{\text{expt}}^r(x, t) - p^r(x, t))^2 dt,$$

where $p_{\text{expt}}^r(x, t)$ is the experimentally determined reflected signal, $p^r(x, t)$ is the reflected wave predicted from Eq. (13). However, because the equations are nonlinear, the analytical method of solving the inverse problem using the conventional least-squares method is tedious. In our case, a numerical solution of the least-squares method can be found which minimizes $U(\phi, \alpha_\infty, \Lambda)$ defined by

$$U(\phi, \alpha_\infty, \Lambda) = \sum_{i=1}^{i=N} (p_{\text{expt}}^r(x, t_i) - p^r(x, t_i))^2, \quad (22)$$

where $p_{\text{expt}}^r(x, t_i)_{i=1,2,\dots,N}$ is the discrete set of values of the experimental reflected signal and $p^r(x, t_i)_{i=1,2,\dots,N}$ is the discrete set of values of the simulated reflected signal. Section VI discusses solution of the inverse problem based on experimental reflected data.

VI. ULTRASONIC MEASUREMENT

In application of this model, some numerical simulations are compared with experimental results. Experiments are performed in air using a broadband Ultran NCT202 transducer with a central frequency of 190 kHz in air and a bandwidth of 6 dB extending from 150 to 230 kHz. This transducer is used simultaneously as a transmitter and receiver to detect the reflected wave. Pulses of 400 V are provided by a 5052PR Panametrics pulser/receiver. The signals received are amplified to 90 dB and filtered above 1 MHz to avoid high frequency noise (energy is totally filtered by the sample in this upper frequency domain by the wave reflected by the second interface). Electronic interference is eliminated by 1000 acquisition averages. The experimental setup is shown in Fig. 8. Signal duration is important in solving the inverse problem; its spectrum must verify the condition of high frequency approximation^{4,6} referred to in Sec. II.

Consider a sample of plastic foam, M1, of two different thicknesses, the first (M1-a) with a thickness of 1.00 ± 0.01 cm and the second (M1-b) 0.62 ± 0.01 cm. Sample M1 was characterized using classic methods^{6,14} given the following physical parameters: $\phi = 0.94 \pm 0.005$, $\alpha_\infty = 1.07 \pm 0.005$, $\Lambda = 200 \pm 5 \mu\text{m}$, $\Lambda' = 600 \pm 15 \mu\text{m}$.

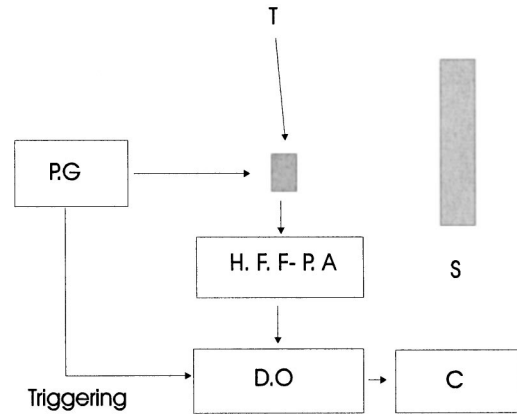


FIG. 8. Experimental setup of the ultrasonic measurements in reflected mode. PG: pulse generator, HF F-PA: high frequency filtering -pre-amplifier, DO: digital oscilloscope, C: computer, T: transducer, S: sample.

Consider the sample M1-a: Figure 9 shows the experimental incident signal generated by the transducer. After solving the inverse problem numerically, we find the following optimized values $\phi = 0.945 \pm 0.005$, $\alpha_\infty = 1.065 \pm 0.005$, $\Lambda = 210 \pm 5 \mu\text{m}$, and $\Lambda' = 630 \pm 15 \mu\text{m}$. Using these values, we present in Figs. 10(a), (b), and (c) the variations in the minimization function U given in Eq. (22) with porosity, tortuosity, and viscous characteristic length, respectively. In Fig. 11, we show a comparison between an experimental reflected signal and simulated reflected signals for the optimized values of porosity, tortuosity, viscous and thermal characteristic lengths. The difference between the two curves is slight, which leads us to conclude that the optimized values of the physical parameters are correct.

Let us now solve the inverse problem for sample M1-b. The experimental incident signal generated by the transducer is shown in Fig. 12. The optimized values of these parameters are $\phi = 0.938 \pm 0.005$, $\alpha_\infty = 1.07 \pm 0.005$, $\Lambda = 170 \pm 5 \mu\text{m}$, and $\Lambda' = 510 \pm 15 \mu\text{m}$. Figure 13 shows a comparison of an experimental reflected signal and a simulated signal obtained by optimization from the inverse problem. Here, again, the correlation of theoretical prediction and experimental data is good.

Using another plastic foam M2 (thickness 1 cm), the incident signal generated by the transducer is given in Fig.

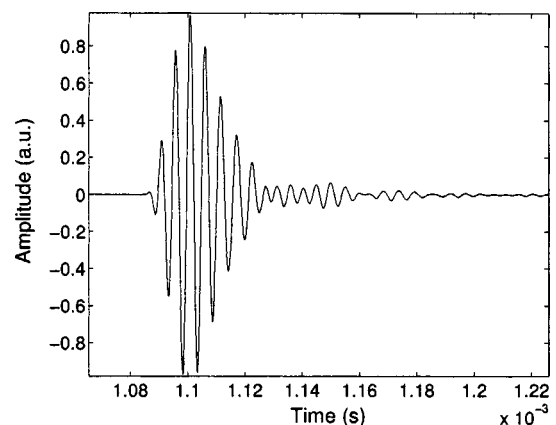


FIG. 9. Experimental incident signal generated by the transducer for the plastic foam sample M1-a.

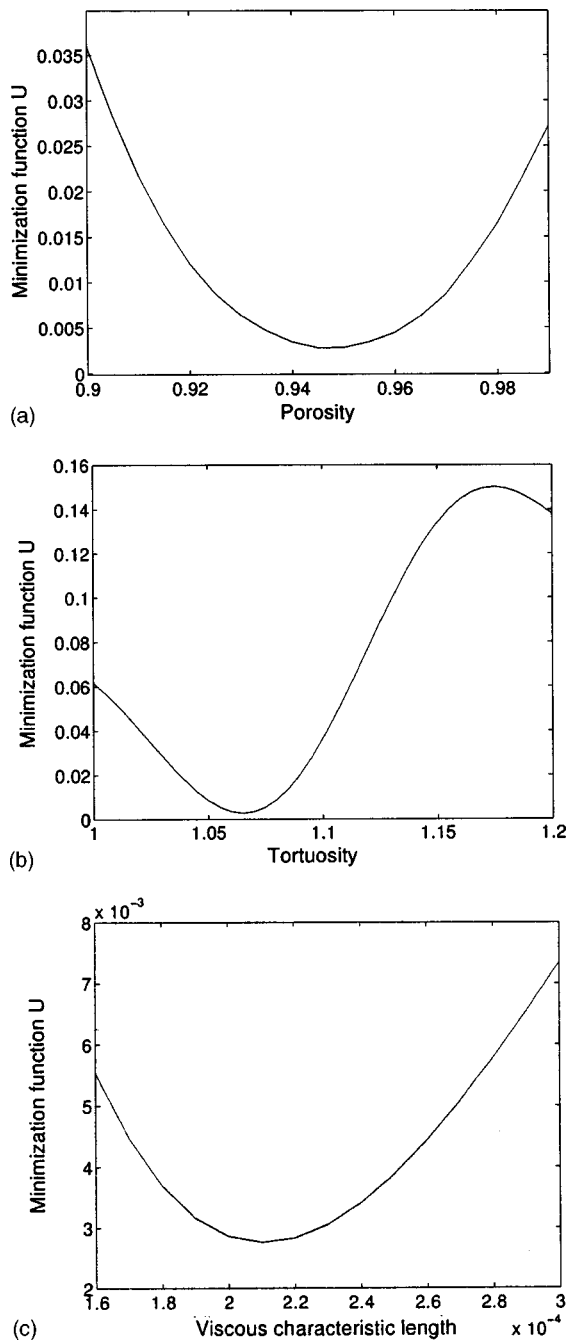


FIG. 10. (a) Variation of the minimization function U with porosity for $\alpha_\infty=1.065$ and $\Lambda=210 \mu\text{m}$ (sample M1-a). (b) Variation of the minimization function U with tortuosity for $\phi=0.945$ and $\Lambda=210 \mu\text{m}$ (sample M1-a). (c) Variation of the minimization function U with viscous characteristic length for $\phi=0.945$ and $\alpha_\infty=1.065$ (sample M1-a).

14. The results, after solving the inverse problem for variation of the minimization function with porosity, tortuosity and viscous characteristic lengths, are: $\phi=0.97\pm 0.005$, $\alpha_\infty=1.075\pm 0.005$, $\Lambda=380\pm 5 \mu\text{m}$, and $\Lambda'=1140\pm 15 \mu\text{m}$. In Fig. 15, we show a comparison of an experimental reflected signal and a reflected simulated signal using optimized values of physical parameters. Classic methods^{6,14} give the following characteristics; $\phi=0.97\pm 0.05$, $\alpha_\infty=1.07\pm 0.005$, $\Lambda=360\pm 5 \mu\text{m}$, and $\Lambda'=1080\pm 15 \mu\text{m}$.

It can be seen that for the three samples, M1-a, M1-b, and M2, the optimized values obtained using this method are

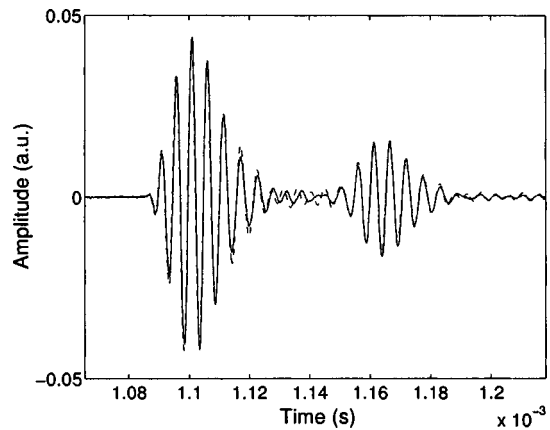


FIG. 11. Comparison between experimental reflected signal (solid line) and simulated reflected signal (dashed line) for the plastic foam sample M1-a ($\alpha_\infty=1.065$, $\phi=0.945$, and $\Lambda=210 \mu\text{m}$).

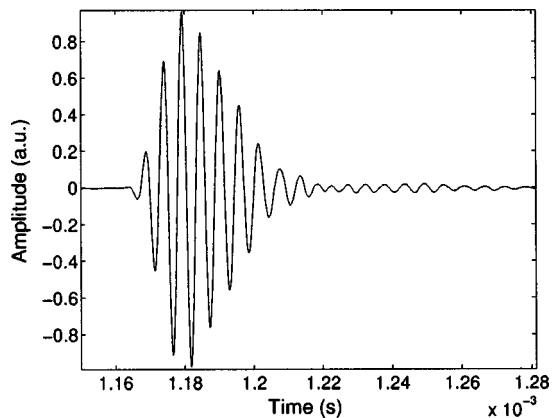


FIG. 12. Experimental incident signal generated by the transducer for the plastic foam sample M1-b.

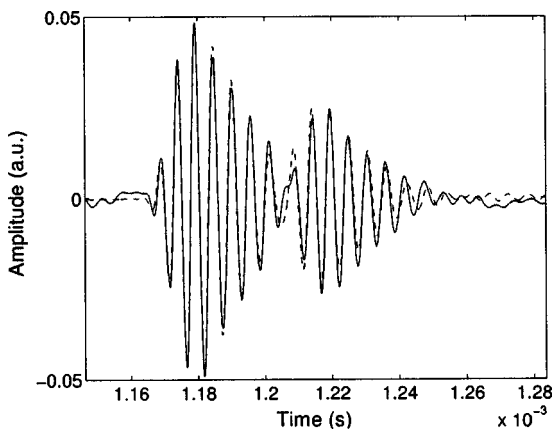


FIG. 13. Comparison between experimental reflected signal (solid line) and simulated reflected signal (dashed line) obtained by optimization from the inverse problem, for the plastic foam sample M1-b ($\alpha_\infty=1.070$, $\phi=0.938$, and $\Lambda=170 \mu\text{m}$).

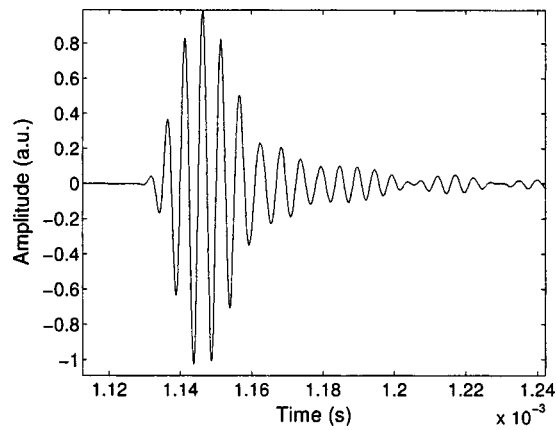


FIG. 14. Experimental incident signal generated by the transducer for the plastic foam sample M2.

close to those produced using classic methods.^{6,14}

This method seems to be efficient for estimating the physical parameters needed to describe sound propagation in air-saturated porous media such as plastic foams. However, when the reflected wave by the second interface cannot be detected experimentally because of strong damping of the acoustic wave inside the porous material, it will be not possible to estimate the transport parameters since the reflected wave at the first interface gives just a relation between α_∞ and ϕ at normal incidence.

VII. CONCLUSION

A method for measuring transport parameters in porous materials simultaneously, using measurements of waves reflected at the first and second interface, has been proposed. This method is based on a temporal model of direct and inverse scattering problems affecting the propagation of transient ultrasonic waves in a homogeneous isotropic slab of porous material with a rigid frame.

Generally, porosity and tortuosity can be evaluated by the wave reflected at the first interface at oblique incidence¹⁴ but this is not possible at normal incidence. Viscous and thermal characteristic lengths can be estimated only by transmitted waves. Porosity cannot be determined from transmitted waves because of its weak sensitivity in this mode. The advantage of the proposed method is that all the parameters can be determined at normal incidence (the ratio between viscous and thermal lengths is fixed as in classical methods^{7,8} based on transmission measurement).

The main principle of this method is the experimental detection of reflected contributions from the first and the second interface of the medium. The properties of these two contributions are used to estimate the four acoustical parameters needed for ultrasonic propagation in porous material with a rigid frame, by solving the inverse problem.

Studying the sensitivity of each reflected wave parameter demonstrates the importance of each contribution (first

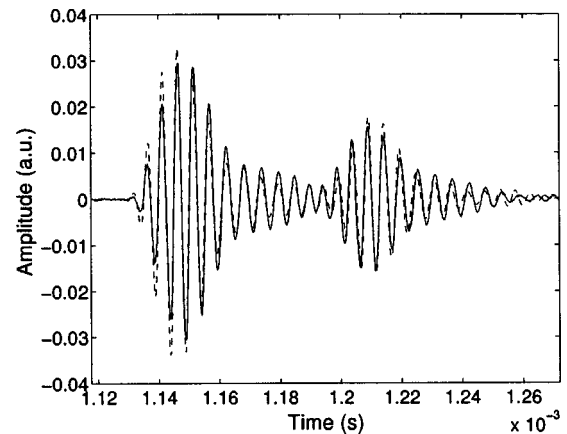


FIG. 15. Comparison between experimental reflected signal (solid line) and simulated reflected signal (dashed line) obtained by optimization of the inverse problem, for the sample M2 ($\alpha_\infty = 1.075$, $\phi = 0.97$, and $\Lambda = 380 \mu\text{m}$).

and second interface) for the inversion. Numerical and experimental validation for weak resistive air-saturated industrial plastic foams is given to validate this method.

¹J. F. Allard, *Propagation of Sound in Porous Media: Modeling Sound Absorbing Materials* (Chapman and Hall, London, 1993).

²K. Attenborough, "On the acoustic slow wave in air-filled granular media," *J. Acoust. Soc. Am.* **81**, 93–102 (1987).

³K. Attenborough, "Models for the acoustical properties of air-saturated granular media," *Acta Acustica* **1**, 213 (1993).

⁴Z. E. A. Fellah and C. Depollier, "Transient acoustic wave propagation in rigid porous media: A time-domain approach," *J. Acoust. Soc. Am.* **107**, 683–688 (2000).

⁵T. L. Szabo, "Time domain wave equations for lossy media obeying a frequency power law," *J. Acoust. Soc. Am.* **96**, 491–500 (1994).

⁶Z. E. A. Fellah, M. Fellah, W. Lauriks, and C. Depollier, "Direct and inverse scattering of transient acoustic waves by a slab of rigid porous material," *J. Acoust. Soc. Am.* **113**, 61–73 (2003).

⁷C. Ayrault, A. Moussatov, B. Castagnède, and D. Lafarge, "Ultrasonic characterization of plastic foams via measurements with static pressure variations," *Appl. Phys. Lett.* **74**, 3224–3226 (1999).

⁸A. Moussatov, C. Ayrault, and B. Castagnède, "Porous material characterization-ultrasonic method for estimation of tortuosity and characteristic length using a barometric chamber," *Ultrasonics* **39**, 195–202 (2001).

⁹M. A. Biot, "The theory of propagation of elastic waves in fluid-saturated porous solid. I. Low frequency range," *J. Acoust. Soc. Am.* **28**, 168–178 (1956).

¹⁰M. A. Biot, "The theory of propagation of elastic waves in fluid-saturated porous solid. II. Higher frequency range," *J. Acoust. Soc. Am.* **28**, 179–191 (1956).

¹¹D. L. Johnson, J. Koplik, and R. Dashen, "Theory of dynamic permeability and tortuosity in fluid-saturated porous media," *J. Fluid Mech.* **176**, 379–402 (1987).

¹²S. G. Samko, A. A. Kilbas, and O. I. Marichev, *Fractional Integrals and Derivatives: Theory and Applications* (Gordon and Breach Science Publishers, Amsterdam, 1993).

¹³Z. E. A. Fellah, M. Fellah, W. Lauriks, C. Depollier, J. Y. Chapelon, and Y. C. Angel, "Solution in time domain of ultrasonic propagation equation in a porous material," *Wave Motion* **38**, 151–163 (2003).

¹⁴Z. E. A. Fellah, S. Berger, W. Lauriks, C. Depollier, C. Aristégui, and J.-Y. Chapelon, "Measuring the porosity and the tortuosity of porous materials via reflected waves at oblique incidence," *J. Acoust. Soc. Am.* **113**, 2424–2433 (2003).